T. A. Godfrey
Research Engineer,
U.S. Army Soldier and Biological
Chemical Command,
Natick Soldier Center,
Mail Stop AMSSB-RSS-M,
Natick, MA 01760-5020
e-mail: tgodfrey@natick-emh2.army.mil
Mem. ASME

J. N. Rossettos
Professor,
Department of Mechanical, Industrial
and Manufacturing Engineering,
Northeastern University,
Boston, MA 02115
Fellow ASME

The Onset of Tear Propagation at Slits in Stressed Uncoated Plain Weave Fabrics

A simple micromechanical model is developed to predict the onset of tear propagation at slit-like damage sites (i.e., a series of consecutive aligned yarn breaks) in biaxially stressed plain weave fabrics under increasing loading. A crucial aspect of the model is the treatment of the frictional slip of yarns near the damage site. Although the actual configuration of slipping regions is complex, the onset of tear propagation in large slits (i.e., more than, say, 35 breaks) is dominated by slip occurring on the first few intact yarns adjacent to the breaks. The assumptions in the mathematical model were motivated by both experimental observations and calculations for key configurations. Analytical results obtained for this simple model exhibit good agreement with experimental results, which are presented for a variety of fabrics with initial slits of 35 and 45 breaks.

Introduction

Bi-axially stressed woven fabrics are used in inflatable and tension structures, parachute canopies, and, increasingly, in geotextile-reinforced geotechnical structures. In end-use, fabrics are often accidentally cut or punctured by a sharp edge or by impact with projectiles. Under sufficiently high remote tension, the local damage provides the starting point for a rapidly propagating tear that results in catastrophic failure of the fabric structure. The problem was recognized in connection with early fabric-covered military aircraft and was addressed by investigators empirically using the *wounded tensile test* (Harrison, 1960). Although the phenomenon has long been known, it has not been the subject of intense fundamental study (i.e., involving multiple investigators over a period of years) and, therefore, progress has been modest.

Installed geotextiles contain holes created by accidental damage, e.g., during compaction of the backfill (Troost and Ploeg, 1990), as well as purposefully made holes to incorporate specific design features of the project. The growth of tears arising from one of these damage sites can lead to sudden failure of the geotechnical structure (Koerner et al., 1987). Given the impact the proper functioning of these structures (e.g., municipal landfills, hazardous waste landfills, levees, etc.) has on the safety and health of local human populations, study of the tear propagation phenomenon is now extremely relevant to the national interest.

Hedgepeth (1961) provided the first micromechanical analysis of a damaged filamentary structure. His analysis, based on shear lag theory, has been applied to fiber/matrix composites, where the matrix transfers the load from broken to unbroken fibers by means of shear. The original work has been the basis of numerous extensions and modifications (see review by Rossettos and Godfrey, 1998). Hedgepeth regarded his shear lag model, where the fibers carry axial loads and the matrix is assumed to carry only shear, to apply to coated woven fabrics as well, where the coating transfers shear between yarns. In bi-axially stressed *uncoated* woven fabrics, load transfer between yarns of a given yarn set is accomplished by rotation of the tensioned crossing yarns in the fabric plane. In this regard, the fabric acts mechanically like a remotely stressed plane pin-jointed net and the shear stiffness is stress-induced, rather than an intrinsic property of the fabric. This stress-stiffening effect has been noted by Christoffersen (1980) and by Topping (1961). The ultimate transfer of load to a given yarn arises through frictional contact between warp and fill yarns at the crossover point.

Christoffersen (1980) derived a general theory for a continuum model of the fabric as a deformable orthotropic plate that allows for elastic stretching along two orthotropic directions and is capable of stress-free deformation in shear. He applied his general theory to the problem of an isolated slit and demonstrated that harmonic problems (Laplace's equation) arise when yarn rotations are small and normal stress is constant in one of the orthotropic directions, as in the case of for the slit interrupting only a single yarn system. It is assumed that sufficient friction or other means prevents yarn slippage at crossover points. This latter assumption is appropriate for coated fabrics, but not for most uncoated fabrics, where yarn slip appears to have an important toughening effect. To capture the frictional slip of discrete yarns, a micromechanical approach is necessary.

The experimental results of Abbott and Skelton (1972) suggest that yarn slip at crossover points may significantly toughen slit-damaged woven fabrics against tear propagation. Abbott and Skelton considered slit damage introduced suddenly into uniaxially loaded fabrics, measuring the critical tension at which tear propagation from the initial slit occurs. In tests of otherwise identical coated and uncoated fabrics, critical tensions for the uncoated specimens were higher by as much as a factor of two. Popova and Iliev (1993) remark on the significant yarn slippage exhibited in experiments on uncoated slitted fabric specimens under uniaxial loading as compared to the behavior of the same fabrics after application of an elastomeric coating.

Godfrey and Rossettos (1998) have introduced a micromechanical modeling approach that addresses the tendency of individual yarns to slip near the damage region. They identify two types of frictional slip that occur near the damage site: type 1 involves slip occurring on yarns broken in the initial slit, and type 2 involves slip occurring on intact yarns in the damage growth path near the tip of the slit. Tear propagation is assumed to occur when the maximum yarn tension in the intact yarn adjacent to the last yarn break approaches the yarn breaking load. Although the basic governing equations are simple, implementing the approach to address a damage configuration involving a practical number of breaks involves considerable difficulty in defining regions on each yarn where slip is occurring. Nonetheless, preliminary experimental results (Godfrey and Rossettos, 1999) demonstrate, through

Contributed by the Applied Mechanics Division of THE AMERICAN SOCIETY OF MECHANICAL ENGINEERS for publication in the ASME JOURNAL OF APPLIED MECHANICS.
Discussion on the paper should be addressed to the Technical Editor, Professor Lewis T. Wheeler, Department of Mechanical Engineering, University of Houston, Houston, TX 77204-4792, and will be accepted until four months after final publication of the paper itself in the ASME JOURNAL OF APPLIED MECHANICS.
Manuscript received by the ASME Applied Mechanics Division, Dec. 2, 1998; final revision, May 11, 1999. Associate Technical Editor: M.-J. Pindera.

correlation with dimensionless parameters in the model, that the present approach captures the essential physics of the phenomenon.

In this work, we adopt a micromechanical modeling approach (Godfrey and Rossettos, 1998) for considering large slits where type 2 slip is assumed to occur on the first few intact yarns at the tip of the slit. For clarity of exposition, some of the original development given in Godfrey and Rossettos (1998) will be summarized here. It will be shown that type 2 slip occurring on the first few intact yarns exerts a dominant influence over the onset of tear propagation in fabrics containing large slits. Experimental results for the onset of tear propagation at 35 and 45 break slits in a variety of biaxially stressed plain weave fabrics are presented and exhibit good agreement with the analytical predictions.

Micromechanical Model

In this section, we summarize the main features of a micromechanics-based mathematical model originally developed in more detail by Godfrey and Rossettos (1998). Consider a plain weave fabric with damage consisting of a slit-like series of consecutive yarn breaks arrayed parallel to the x_2-coordinate direction at $x_1 = 0$, where the x_1x_2-coordinate system is aligned with the yarn directions. The microstructural geometry and nomenclature pertaining to the damaged fabric is indicated in Fig. 1. The slit interrupts only number one (# 1) yarns, referring to yarns parallel to the x_1 and x_2-directions as # 1 and number two (# 2) yarns, respectively. The plain weave unit cell dimensions are y_{01} along the x_1-axis (the spacing of the # 2 yarns) and y_{02} along the x_2-axis (the spacing of the # 1 yarns). Remote biaxial membrane stresses (i.e., having dimensions of force/length) are applied to the fabric such that the stress in the x_2 direction, T_2, is held constant while the stress in the x_1 direction, T_1, is increased quasi-statically. The global configuration of the damage and remote loading is shown in Fig. 2. At the microstructural level, the membrane stresses are viewed as individual remote yarn tensions such that # 2 yarns are under constant remote tensions F_2^* and # 1 yarns are under quasistatically increasing remote tensions p (i.e., $T_1 = p/y_{02}$, $T_2 = F_2^*/y_{01}$). As x_1-direction loading increases, the # 1 yarns exhibit displacements in the x_1-direction and the # 2 yarns exhibit x_1-direction displacements and small rotations in the fabric plane (Fig. 3). With continued increasing loading, the # 1 and # 2 yarns may be observed to slip at crossover points in a region near the

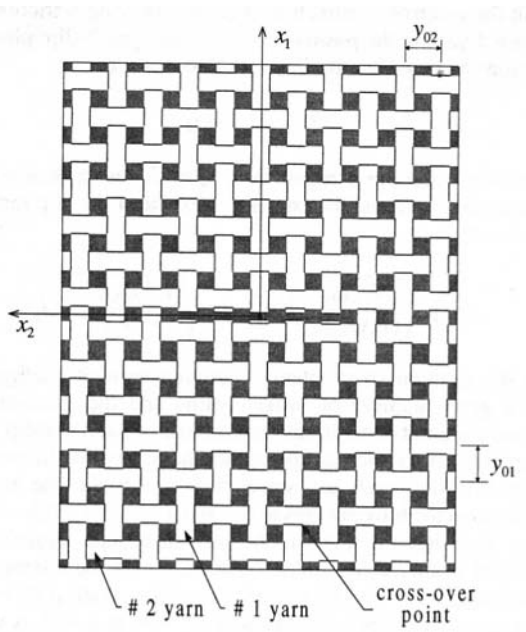

Fig. 1 Microstructural geometry of fabric containing five break slit-like damage

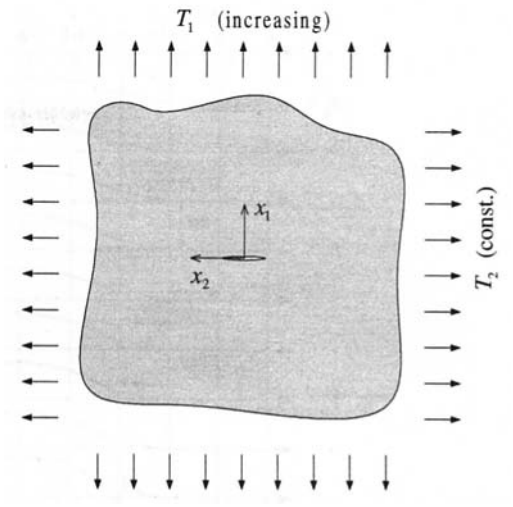

Fig. 2 Configuration of biaxial remote stresses on damaged fabric

breaks (Fig. 4). When p reaches a critical value p_c, the initial slit damage propagates through rupture of the intact # 1 yarns on either side of the breaks roughly along the line $x_1 = 0$.

Appropriate differential equations that describe the equilibrium of yarns in regions where slip at crossover points occurs, and in the region where slip does not occur, can easily be derived (Godfrey and Rossettos, 1998). For instance, in the region where crossover point slip does not occur, equilibrium of the # 1 yarns can be derived by taking into account the load transfer to the # 1 yarns that occurs due to the rotated tensioned # 2 yarns in the fabric plane. For small rotations, the angles are indicated in Fig. 3(*b*). The component of the # 2 yarn tension along the # 1 yarn can then be written. Introduce u_n^j as the x_1-displacement of the jth crossover point on the nth # 1 yarn, where the reference state for displacements are the positions of points on an otherwise identical stressed fabric *without damage*. In the development of the mathematical model, analytical and experimental curves (Godfrey and Rossettos, 1998) of yarn force versus strain in the x_1-direction for Kevlar® and Dacron® fabrics have shown good agreement, thereby lending validity to the crimp interchange mechanics used in the model. For sufficiently high values of the loading, p, the # 1 yarns are assumed to be in a nearly straightened out condition, and display an effective constant axial stiffness property $(EA)_{\text{eff}}$ having the dimension of force. Rotation of the # 2 yarns is represented by relative displacements at points on adjacent # 1 yarns. Considering the crossover point unit cell as a free body, Fig. 3(*b*), the component of force in the x_1-direction acting on the # 2 yarn entry and exit boundaries will be $F_2^*(u_{n-1}^j - u_n^j)/y_{02}$ and $-F_2^*(u_n^j - u_{n+1}^j)/y_{02}$. Therefore, equilibrium of the jth crossover unit cell in the x_1-direction is written as

$$F_{1n}^{j+1} - F_{1n}^j + \frac{u_{n-1}^j - 2u_n^j + u_{n+1}^j}{y_{02}} F_2^* = 0. \tag{1}$$

Replace the jth and $j+1$th F_{1n} terms with differences of crossover point displacements $(EA)_{\text{eff}}(u_n^j - u_n^{j-1})/y_{01}$ and $(EA)_{\text{eff}}(u_n^{j+1} - u_n^j)/y_{01}$, respectively. These terms are strains on either side of crossover point j multiplied by $(EA)_{\text{eff}}$. Equation (1) becomes

$$\frac{(EA)_{\text{eff}}}{y_{01}}(u_n^{j-1} - 2u_n^j + u_n^{j+1}) + \frac{F_2^*}{y_{02}}(u_{n-1}^j - 2u_n^j + u_{n+1}^j) = 0. \tag{2}$$

Smearing out the interaction with the # 2 yarns and regarding u_n as a continuous function of position x_1, this equilibrium equation, for nonslipping yarns, can then be written as

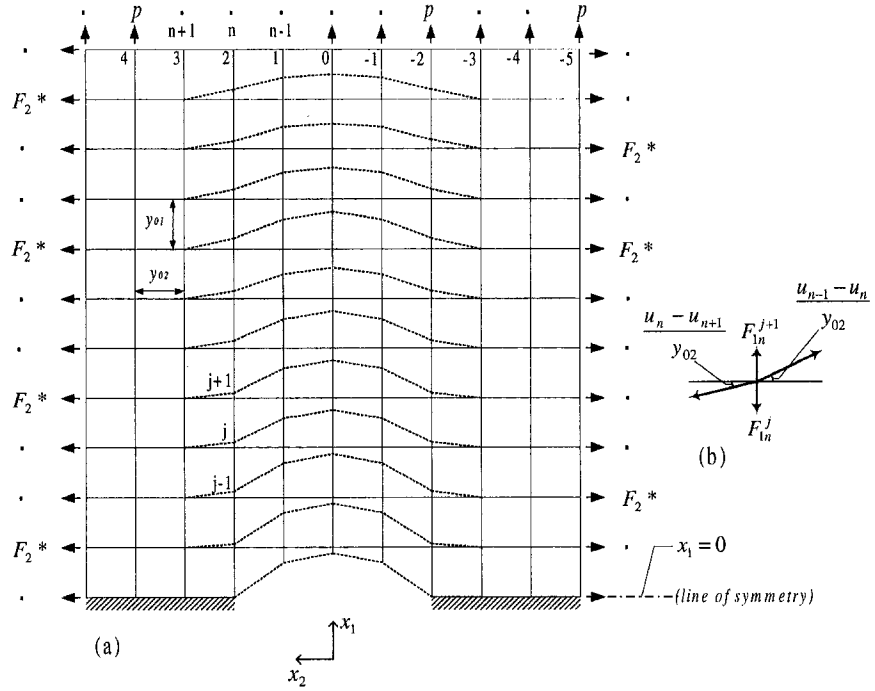

Fig. 3 (*a*) Geometry of damaged fabric indicating the elastic (nonslipping) deformation. Highly schematic, only yarn centerlines are shown. Breaks in # 1 yarns, dashed lines represent deformed # 2 yarns. (*b*) Equilibrium of the *j*th crossover point unit cell.

$$\frac{d^2u_n}{dx_1^2} + \frac{F_2^*}{(EA)_{\text{eff}} y_{01} y_{02}} (u_{n-1} - 2u_n + u_{n+1}) = 0. \tag{3}$$

Equation (3) is written in dimensionless form as

$$U_n'' + U_{n-1} - 2U_n + U_{n+1} = 0 \tag{4}$$

using the following nondimensionalization:

$$x_1 = \sqrt{\frac{(EA)_{\text{eff}} y_{01} y_{02}}{F_2^*}}\, \xi, \quad u_n = p \sqrt{\frac{y_{01} y_{02}}{(EA)_{\text{eff}} F_2^*}}\, U_n \tag{5}$$

where primes denote differentiation with respect to ξ.

Crossover point slip is assumed to occur in a region near the breaks, $0 < x_1 < l_n$, where l_n denotes the extent of the slip region on the nth # 1 yarn. In the slipping region, the yarn is assumed to experience a periodic array of frictional tractions f of constant value (simple slip assumption (Godfrey and Rossettos, 1998)), the period corresponding to the crossover point spacing. The equilibrium equation can be written as

$$\frac{d^2u_n}{dx_1^2} \mp \frac{f}{(EA)_{\text{eff}} y_{01}} = 0 \tag{6}$$

where the minus sign applies for slip of a broken yarn and the plus sign applies for slip occurring on an intact yarn. It is noted that yarns that are broken (# 1 yarns) will slip in the positive x_1-direction relative to the crossing # 2 yarns (Fig. 4), thereby incurring a friction force in the negative x_1-direction (type 1 slip: minus sign). In the slip that occurs on an intact yarn, the # 2 yarns slip in the positive x_1-direction (Fig. 4), applying a friction force on the # 1 yarn in the positive x_1-direction (type 2 slip: plus sign). Equation (6) is written in dimensionless form as

$$U_n'' \mp \hat{f} = 0 \tag{7}$$

where slip occurs in a region $0 < \xi < \hat{l}_n$ and a dimensionless loading parameter and dimensionless extent of the slip region are introduced:

$$f = p \sqrt{\frac{F_2^* y_{01}}{(EA)_{\text{eff}} y_{02}}}\, \hat{f}, \quad l_n = \sqrt{\frac{(EA)_{\text{eff}} y_{01} y_{02}}{F_2^*}}\, \hat{l}_n. \tag{8}$$

In the solution of problems involving various configurations with a given number of broken yarns and the associated slip regions, continuity conditions between the slip and nonslip regions are applied, in addition to appropriate boundary conditions. Since the broken yarn ends are stress free at the slit, the boundary condition on the broken yarns at $\xi = 0$ is $U_n' = -1$. The -1 is due to the fact that the sum of the reference state strain and the additional strain du_n/dx_1 must vanish at $\xi = 0$; the reference state strain is $du_R/dx_1 = p/(EA)_{\text{eff}}$ and, using (5), get $dU_R/d\xi = 1$. For intact yarns, symmetry requires that $U_n = 0$ at $\xi = 0$. A uniform strain is assumed far from the breaks, therefore, for all yarns we require that $U_n' = 0$ at $\xi = \infty$.

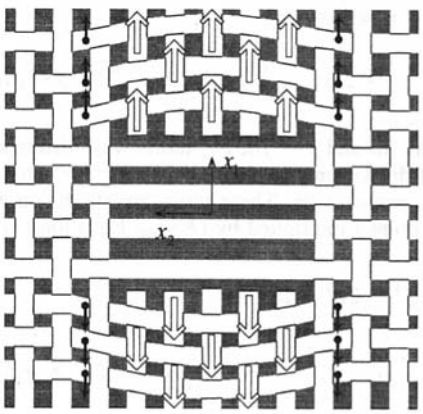

Fig. 4 Yarn slip and deformation pattern near slit. White arrows indicate motion of broken # 1 yarns in type 1 slip. Black arrows indicate motion of # 2 yarns in type 2 slip. Highly schematic.

Application to Large Slits—Type 2 Slip

The essential mechanisms of the model are depicted by the equilibrium equations, i.e., (4) and (7), and appropriate boundary and continuity conditions as discussed above. Although the basic equations are simple, the opportunity for each yarn near the damage site to slip over a unique slip extent, l_n, creates significant difficulty in implementing the model to treat specific numbers of breaks. For larger slits, the actual configuration of the slipping regions may be expected to become increasingly complex. For predicting the onset of tear propagation, our interest is in the stress concentration in the first intact yarn at the tip of the slit. Since knowledge of the complete deformation field of the fabric under increasing load is not our goal, we exploit simplifications designed to approximate the fabric's behavior in the immediate vicinity of the first intact yarn at loads corresponding to the onset of tear propagation.

As previously mentioned, type 2 slip is the slip that occurs when a rotated crossing yarn slips in the positive x_1-direction at a crossover point with an intact yarn, straightening the kink that occurs at the crossover point to a degree (Fig. 4). Type 1 slip is the slip that occurs on broken yarns as they displace relative to the crossing yarns, moving away from the initial line of breaks (Fig. 4). For slits involving small numbers of breaks, where high remote loads may be attained, type 1 slip may be easily observed in testing because the slip displacements are significant; the broken ends of the yarns often slip far enough to disengage from their interlacings with several crossing yarns.

Consider the damaged fabric under a slowly increasing remote yarn load p starting from zero. Initially, for large slits, the fabric behaves elastically (no slip) until p attains the threshold value p_{limit}, when type 2 slip begins along the first intact # 1 yarn at the tip of the slit. As the load is increased further, the type 2 slip extent grows and a second load threshold is reached when type 1 slip begins at the outermost broken yarn. For further increases in the load, the type 1 slip extent will increase approximately linearly with the load, as shown by calculations in Godfrey and Rossettos (1998), but, for some regime of load, the type 1 slip extent will remain significantly smaller than the type 2 slip extent. Since, for increasingly large slits, tear propagation can be expected to occur at smaller values of p (larger stress concentrations), the loading regime in which either type 2 slip occurs alone, or occurs over a much larger extent than type 1 slip, encompasses the loads over which tear propagation occurs in many stressed fabrics. Post-test inspection of experimental specimens confirms this expectation, where little evidence of type 1 slip is exhibited by the most damage sensitive fabrics.

Comparison of the post-test permanent deformation patterns in the vicinity of slit damage in fabric specimens with small and large slits supports the notion that the type 2 slip mechanism becomes increasingly important in larger slits. Specimens of a continuous filament polyester fabric with damage consisting of three (small slit) and 45 (large slit) consecutive aligned fill yarn breaks were tested under the considered bi-axial loading. The fabric, and the method and conditions of the biaxial testing, are described in the experimental section of this paper. The polyester fabric is the most damage tolerant of those studied here and, therefore, exhibits the largest and most well developed slip regions. The post-test configuration of the three break specimen, after removal of the external loads, is exhibited in Fig. 5. As can be seen, tear propagation *did not* occur at the initial damage site; the test ended in a "jaw break" type failure. The deformation pattern provides clear evidence of substantial type 1 slip: the cut ends of the three broken yarns have displaced far enough to disengage from interlacings with seven or eight # 2 yarns; the three broken yarns exhibit a distinct wiggly appearance for some length starting at the cut ends, suggestive of a slipped yarn region adjacent to an unslipped region of the broken yarns further away from the origin. The overall waviness exhibited by all # 1 yarns in the figure is due to the general plastic deformation of the # 1 yarns in the specimen caused

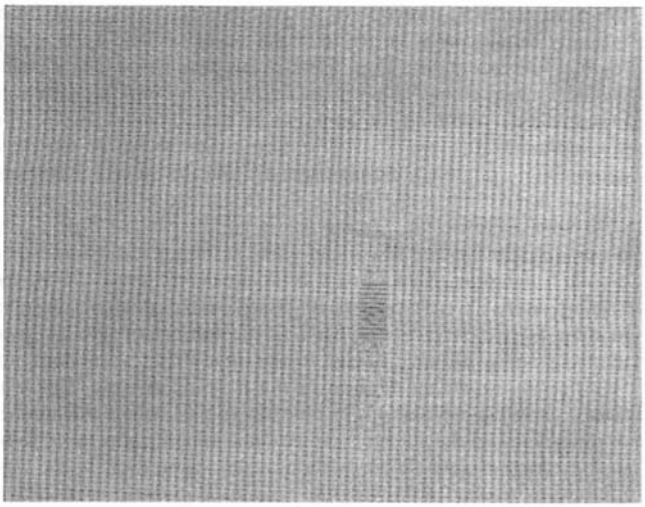

Fig. 5 Post-test permanent deformation pattern in three break specimen, polyester fabric

by the high value of the remote tension, p, experienced in this test. Examination of the # 2 yarns in this specimen reveals that they remain essentially straight and parallel to the x_2-coordinate axis in the vicinity of the local damage, a fact that is consistent with the hypothesis that very little, if any, slip occurred at crossover points along the intact yarns (type 2 slip). The post-test configuration of the 45 break specimen, after removal of external loads, is exhibited in Fig. 6. This test ended in tear propagation, as evidenced by the frayed looking yarn ends resulting from the rupture of the initially intact # 1 yarns along the line $x_1 \cong 0$. The displacement of the cut yarn ends seen here, similar to that seen in the three break specimen, also indicates substantial type 1 slip. In the 45 break case, however, the # 2 yarns are permanently curved such that, as they approach their crossover points with the broken # 1 yarns, the # 2 yarns move away from the line of initial breaks. Crossover points on any particular # 2 yarn, where it is interlaced with the 45 initially broken # 1 yarns, are seen to lie at greater distances from the line $x_1 \cong 0$ than cross-over points where the # 2 yarn is interlaced with the initially intact # 1 yarns (except in the region of complicated deformation very near the cut ends). This pattern can be seen in the entire field of view of Fig. 6. The occurrence of type 2 slip along several intact # 1 yarns at the tips of the slit provides a plausible explanation of the observed deformation pattern. The fact that the pattern extends to the edge of the figure suggests that

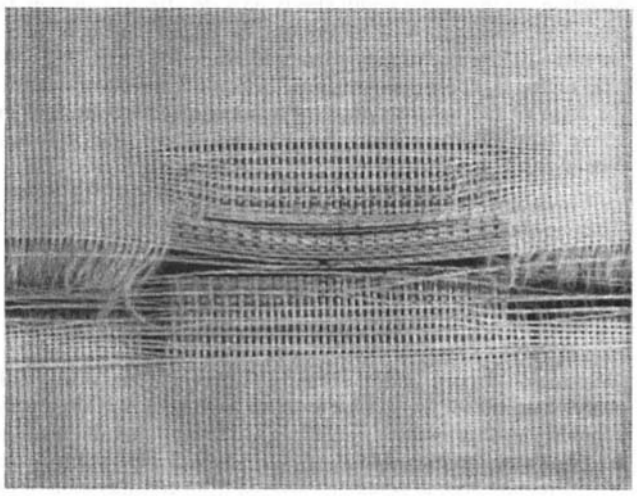

Fig. 6 Post-test permanent deformation pattern in 45 break specimen, polyester fabric

the extent in the x_1-direction of the region experiencing type 2 slip is likely significantly larger than the extent of the type 1 slip region. Taken together, Figs. 5 and 6 suggest that, as the considered slit size becomes larger, type 2 slip becomes the predominant inelastic mechanism in the response of the damaged fabric. The predominance of type 2 slip in large slits is apt to be most applicable to relatively damage sensitive fabrics, where tear propagation occurs before the type 1 slip extent grows significantly.

In what follows, we assume for large slits, that a type 2 slip occurs in only the first few intact yarns at the tip of the slit over a common extent, l. Type 1 slip is assumed *not to occur* on the broken yarns. These simple assumptions on slip configuration are justified by two observations. First, the occurrence of type 2 slip on yarns at some distance ahead of the first intact yarn does not significantly affect the tension in the first intact yarn. This was demonstrated in calculations by Godfrey (1998), where the number of intact yarns at the slit tip assumed to be slipping was taken to be in the range of four to ten without affecting tension in the first intact yarn. Second, following the discussion given in the previous paragraphs, it can be shown for large slits a posteriori from results of the calculation, using (7), that, for values of the remote load that are of interest, type 1 slip either will not occur or its extent will be small (note that, if $U''_N(0^+) \le \hat{f}$, where yarn N is the last broken yarn, no type 1 slip will occur). This suggests that type 2 slip will have the primary influence over the stress concentration in the first intact yarn.

We consider a finite width configuration of $2q + 1$ # 1 yarns with $2N + 1$ consecutive aligned breaks (slit) centered at the zeroth yarn. Yarns in the positive x_2 half-plane are numbered so that n equals 1 to q. Yarns in the negative x_2 half-plane are numbered -1 to $-q$. The series of breaks is symmetrical about the center yarn, so that, concerning ourselves only with nonnegative n, yarns numbered $0 \le n \le N$ are broken and yarns numbered $n > N$ are intact. Because of symmetry, we need only consider equations for yarns $n = 0$ to $n = q$.

The fabric is divided into regions I, $0 < \xi < \hat{l}$, where type 2 slip is occurring on yarns $n = N + 1$ to $n = N + s$, and II, $\xi \ge \hat{l}$, where no slip is occurring. In the analysis, we will arbitrarily take s to be four, for definiteness. As mentioned, varying the value of s from four to ten has an insignificant effect on the stress concentration in the first intact yarn (Godfrey, 1998). The value of q is assumed to be sufficiently large such that the behavior of the finite width configuration closely approximates that of an infinite fabric with an isolated slit. Similar studies in composite sheets containing matrix yield zones near the slit tip (Rossettos and Shishesaz, 1987; Rossettos and Olia, 1995), where the structure of the equations is the same (Rossettos and Godfrey, 1998) and the slip zone in fabrics plays an analogous role as the matrix yield zone in composites, have shown exponential decay in the width direction, so that finite width sheets provide effective models for the infinite sheet problems. Therefore, the displacements of yarn q are taken to be those of the undamaged reference, i.e., $U_q(\xi) = 0$.

In region II (nonslipping region), the equilibrium equations have the form of (4), where symmetry about the center yarn and the above assumption regarding the qth yarn, lead to the following special forms for yarns 0 and $q - 1$, written as

$$U''_0 - 2U_0 + 2U_1 = 0 \tag{9}$$

and

$$U''_{q-1} + U_{q-2} - 2U_{q-1} = 0, \tag{10}$$

respectively.

In region I, (4), and the special forms (9) and (10), hold everywhere except for yarns $n = N$ through $n = N + 5$. For the slipping yarns, $N + 1 \le n \le N + 4$, the equilibrium equations are (7) where the plus sign is taken for type 2 slip. Yarns N and $N + 5$ require special equations derived from consideration of the equilibrium and deformation of that portion of a crossing (# 2) yarn that spans the crossover points on # 1 yarns from yarn N to yarn $N + 5$. The derivation proceeds as follows. It is assumed that the # 2 yarns behave as classical taut strings under transverse loads, f, at the four slipping crossover points. The displacement of the crossing (# 2) yarns in the x_1-direction at the slipping crossover points is denoted by δ_n, $N + 1 \le n \le N + 4$. Force equilibrium in the x_1-direction is written for each of the slipping crossover points on the # 2 yarns, where force components arise from the small rotations of the tensioned # 2 yarns and the small rotation angles are indicated by differences of displacements, i.e., $(\delta_{n-1} - \delta_n)/y_{02}$. This leads to a system of four linear equations for the four unknown # 2 yarn displacements: $(u_N - 2\delta_{N+1} + \delta_{N+2})F_2^*/y_{02} = f$, $(\delta_{N+1} - 2\delta_{N+2} + \delta_{N+3})F_2^*/y_{02} = f, \ldots, (\delta_{N+3} - 2\delta_{N+4} + u_{N+5})F_2^*/y_{02} = f$. Using (5) to nondimensionalize both # 1 and # 2 displacements (i.e., u_n and δ_n), and (8) to nondimensionalize f, the four equations take the form: $U_N - 2\Delta_{N+1} + \Delta_{N+2} = \hat{f}$, $\Delta_{N+1} - 2\Delta_{N+2} + \Delta_{N+3} = \hat{f}$, $\Delta_{N+2} - 2\Delta_{N+3} + \Delta_{N+4} = \hat{f}$, and $\Delta_{N+3} - 2\Delta_{N+4} + U_{N+5} = \hat{f}$, where the Δ_n are the dimensionless displacements of the # 2 yarn crossover points. Observing that the equation for the Nth # 1 yarn will have the form $U''_N + U_{N-1} - 2U_N + \Delta_{N+1} = 0$, and that of the $N + 5$th # 1 yarn will have the form $U''_{N+5} + \Delta_{N+4} - 2U_{N+5} + U_{N+6} = 0$, the solution for Δ_{N+1} and Δ_{N+4}, obtained from the four equations for the Δ_n, may be substituted into the equations for the Nth and $N + 5$th # 1 yarn to obtain

$$U''_N + U_{N-1} - \tfrac{6}{5}U_N + \tfrac{1}{5}U_{N+5} = 2\hat{f} \tag{11}$$

and

$$U''_{N+5} + \tfrac{1}{5}U_N - \tfrac{6}{5}U_{N+5} + U_{N+6} = 2\hat{f}. \tag{12}$$

As previously discussed, the boundary conditions may be written for intact and broken yarns as

$$U_n(0) = 0,\ n \ge N + 1; \quad U'_n(0) = -1,\ n \le N; \tag{13}$$

at $\xi = 0$ and as

$$U'_n(\infty) = 0 \tag{14}$$

for all yarns, $0 \le n \le q - 1$, at $\xi = \infty$. Since all yarns are continuous at $\xi = \hat{l}$, the following continuity conditions hold, where roman numeral subscripts I and II refer to the solution in regions I and II, respectively,

$$U_{\mathrm{I}n}(\hat{l}) = U_{\mathrm{II}n}(\hat{l}); \quad U'_{\mathrm{I}n}(\hat{l}) = U'_{\mathrm{II}n}(\hat{l}). \tag{15}$$

An additional continuity condition arises from the assumption that slipping is approached in a continuous fashion. This may be illustrated by considering a point at $x_1 = a$ on yarn $n = N + 1$. As the remote load p is increased, a value of p is reached that just starts slip with the extent $l = 0^+$. As the load is increased further, the slip extent l increases, but, as long as $l < a$, no slip occurs at

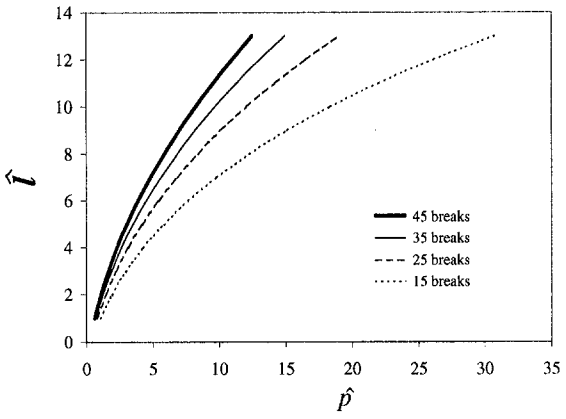

Fig. 7 Behavior of type 2 slip extent, $\hat{l}$, with increasing dimensionless applied load, $\hat{p}$

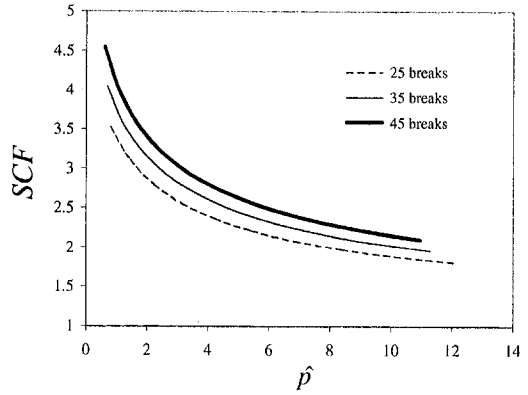

Fig. 8 SCF versus $\hat{p}$ for slits of various numbers of breaks, large-slit analysis

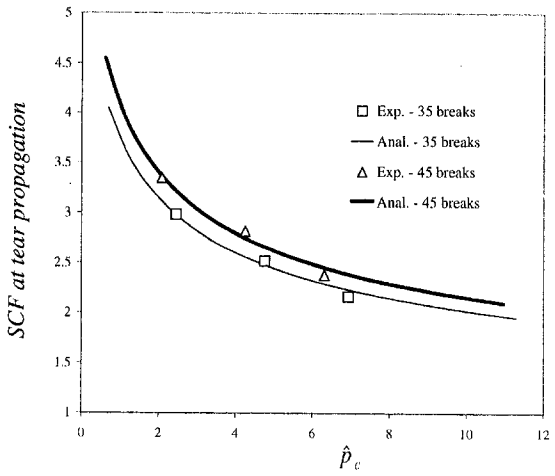

Fig. 9 Comparison of analytical and experimental SCF_{tp} versus $\hat{p}_c$ behavior for 35 and 45 break slits

the point $x_1 = a$. During this time, the frictional forces at the nonslipping crossover points in the neighborhood of $x_1 = a$ increase continuously, until they reach a maximum value of f (on the verge of slip) as the slip extent l approaches a. Therefore, the frictional force on yarn $N + 1$ (proportional to U''_{N+1}) is taken to be continuous at $x_1 = l$, which may be stated in the dimensionless variables, using (4) and (7), as

$$\{U_N - 2U_{N+1} + U_{N+2}\}_{II}|_{\xi=\hat{l}} = \hat{f}. \tag{16}$$

The system of second order differential equations, namely (4), (9), (10), (11), and (12), for the nonslipping yarns in region I may be written in matrix form as

$$\mathbf{U}''_I - \mathbf{L}\mathbf{U}_I = \mathbf{Q} \tag{17}$$

where $\mathbf{L}$ is banded, $\mathbf{U}_I^T = [U_0, U_1, \ldots, U_N, U_{N+5}, U_{N+6}, \ldots, U_{q-2}, U_{q-1}]$, and the elements of $\mathbf{Q}$ are all zero except the $N + 1$th and $N + 2$th element (corresponding to equations for yarns N and $N + 5$), which are $2\hat{f}$. A homogeneous solution to (17) is assumed in the form $\mathbf{U}_I = \mathbf{R}e^{\lambda\xi}$, where $\mathbf{U}_I$ and $\mathbf{R}$ are vectors of order $q - 4$. The resulting eigenvector problem, $(\mathbf{L} - \lambda^2\mathbf{I}) = \mathbf{0}$, leads to eigenvalues λ_i^2 and eigenvectors $\mathbf{R}^i$. The solution $\mathbf{U}_I$ can be written by the superposition of eigenvectors as the expansion

$$\mathbf{U}_I = \sum_{i=1}^{q-4} \mathbf{R}^i(B_i e^{-\lambda_i\xi} + C_i e^{\lambda_i\xi}) + \mathbf{U}_P \tag{18}$$

where the particular solution, $\mathbf{U}_P$, has been added to satisfy (17). The solution for the slipping yarns in region I, which involves (7), is

$$U_{In} = -\frac{\hat{f}}{2}\xi^2 + A_n\xi, \quad N + 1 \le n \le N + 4. \tag{19}$$

The system of second-order differential equations, namely (4), (9), and (10), for region II may similarly be written in matrix form and the solution may be written as the eigenvector expansion

$$\mathbf{U}_{II} = \sum_{i=1}^{q} \mathbf{Y}^i D_i e^{-\gamma_i\xi} \tag{20}$$

where the $+\gamma_i$ have been discarded to satisfy (14), $\mathbf{U}_{II}$ and $\mathbf{Y}$ are vectors of order q, and $\mathbf{U}_{II}^T = [U_0, U_1, \ldots, U_{q-2}, U_{q-1}]$.

To complete the solution process, we select values for the slip extent, $\hat{l}$, and determine the values of the constants (i.e., A_i, B_i, C_i, and D_i) and the parameter, $\hat{f}$, using the boundary conditions, (13), and the continuity conditions, (15) and (16). Observing from (8) that the parameter $\hat{f}$ is inversely proportional to the applied load, p, we introduce a dimensionless applied load, $\hat{p}$, which we define as $\hat{p} = \hat{f}^{-1}$, in the interest of clarity in the presentation and interpretation of the results.

Analytical Results—Type 2 Slip

As indicated above, the behavior of type 2 slip extent, $\hat{l}$, with increasing dimensionless applied load, $\hat{p}$, may be obtained by selecting values of $\hat{l}$ and solving the defined boundary value problem to yield $\hat{f}$, where $\hat{p} = \hat{f}^{-1}$. In Fig. 7, $\hat{l}$ is plotted against $\hat{p}$ for various numbers of breaks. It is seen that larger slits (i.e., involving greater numbers of breaks) yield significantly greater slip extents for given values of $\hat{p}$.

The stress concentration factor (SCF) is defined here as the ratio of the maximum tension in the intact yarn adjacent to the yarn break at the tip of the slit to the remote applied load, p_{max}/p. Using

Table 1 Fabric properties

Fabric	# 1 yarn system	y_{01}, cm	y_{02}, cm	p_u, N	$(EA)_{eff}$, N	F_2^*, N	f, N
Cotton	fill	0.0334	0.0379	1.93	32.3	0.569	0.0328
Polyester, continuous filament	fill	0.0348	0.0686	6.36	23.9	0.888	0.0582
Cotton/polyester blend	fill	0.0334	0.0391	2.27	40.4	0.569	0.0356
Cotton/polyester blend	warp	0.0391	0.0334	2.50	71.2	0.388	0.0166

Table 2 Tear propagation results for 35 and 45 break slits

Fabric	# 1 yarn system	35 break slit $\hat{p}_c$	35 break slit SCF_{tp}	45 break slit $\hat{p}_c$	45 break slit SCF_{tp}
Cotton	fill	2.45 (0.612)†	2.98 (0.364)	—	—
Polyester, continuous filament	fill	6.94 (0.944)	2.16 (0.018)	6.31 (0.883)	2.38 (0.080)
Cotton/polyester blend	fill	—	—	2.09 (0.449)	3.35 (0.155)
Cotton/polyester blend	warp	4.76 (0.571)	2.52 (0.144)	4.25 (0.551)	2.82 (0.212)

† Standard deviations indicated in parenthesis.

the displacement reference and the nondimensionalization scheme, it is straightforward to show that the SCF can be written as SCF = $U'_{N+1}(0) + 1$. The SCF due to slits containing various numbers of breaks is plotted against $\hat{p}$ in Fig. 8.

Experiments

To investigate the predictive ability of the simple micromechanical large-slit model, a number of plain weave fabrics have been studied experimentally. Particular aspects of the experimental methods are described in more detail by Godfrey and Rossettos (1999), where preliminary results for 26 break slits are given. The methods used to obtain the present results differ only in that an improved specimen is used that provides a larger (15 cm × 15 cm) bi-axially stressed region.

It is assumed that the onset of tear propagation occurs when the maximum yarn tension in the fabric, p_{max}, occurring in the $N + 1$th (first intact) yarn attains the value of the in situ ultimate breaking load of the # 1 yarn, p_u. The SCF in a particular fabric, under specific crossing yarn tension F_2^*, for a slit consisting of a given number of # 1 yarn breaks, takes on a special value at the onset of tear propagation, which we denote SCF_{tp}. Since the applied load has the value p_c (*p critical*) at the instant of tear propagation, we may write SCF_{tp} as $SCF_{tp} = p_u/p_c$. The SCF versus $\hat{p}$ behavior, exhibited in Fig. 8, may be interpreted as representing the SCF_{tp} versus $\hat{p}_c$ behavior of fabrics, where $\hat{p}_c$ is the dimensionless applied load at the onset of tear propagation, written, using (8), as

$$\hat{p}_c = \frac{p_c}{f}\sqrt{\frac{F_2^* y_{01}}{(EA)_{\text{eff}} y_{02}}}. \tag{21}$$

We will present our experimental results, which are essentially values of p_c measured in a variety of stressed fabrics for slits of 35 and 45 breaks, through the dimensionless parameters, SCF_{tp} and $\hat{p}_c$.

The selection of 35 and 45 breaks for study was motivated by previous work with 26 breaks and the desire to study larger damage sizes. Much larger sizes were not considered because of limitations in existing experimental means, as well as the concern that very large slits may violate some of the fundamental modeling assumptions, such as the small # 2 yarn rotation assumption.

The experimental set-up uses cruciform-shaped specimens where a fixed stress is applied in the x_2-direction (a force on each # 2 yarn of F_2^*) using an air cylinder actuated frame and a varying stress (from zero to high values) is applied in the x_1-direction by a servo-hydraulic test machine. In tear propagation experiments, the initial slit-like damage is created in the center of the specimen by carefully cutting consecutive # 1 yarns using a sharp razor. The damaged specimen is mounted in the frame and F_2^* is applied. The value of the remote load p is increased monotonically from zero until tear propagation occurs; the maximum value of p is taken to be p_c.

To evaluate the dimensionless parameters, the values for y_{01}, y_{02}, p_u, and $(EA)_{\text{eff}}$ are determined for the particular fabric and orientation under consideration. In addition, the value of f is determined for the specific value of F_2^* to be used in the tear propagation tests. Measurements of the in situ yarn stiffness and strength, $(EA)_{\text{eff}}$ and p_u, respectively, are made using uniaxially loaded "ravel strip" specimens. The value of $(EA)_{\text{eff}}$ is determined from the slope of the load/strain curve in the region where the loaded yarns have straightened out. The crossover point slip frictional force, f, is measured indirectly using a cruciform specimen with a small number of breaks (five to seven) observed under magnification on a video monitor, where the deflections of the # 2 yarns caused by interaction with slipping # 1 yarns are used to calculate f. The frictional forces balance components of the forces in the tensioned crossing (# 2) yarns as they rotate through small angles. These angles, and therefore the frictional forces, can be calculated from the deflections. The selection of five to seven breaks for the measurements is a trade-off between two competing effects: Smaller numbers of breaks yield less deformation in the # 2 yarns and, therefore, make measurements more difficult; using larger numbers of breaks introduces the possibility that not all of the broken # 1 yarns will be slipping simultaneously at crossover points on the # 2 yarn selected for measurement. Attempts to measure f with larger numbers of breaks (fifteen) resulted in lower values, which is consistent with the notion that not all crossover points were contributing the maximum frictional force associated with slip.

A 100 percent cotton staple yarn fabric, a cotton/polyester blend staple yarn fabric, and a continuous multifilament polyester yarn fabric are studied here. All fabrics are plain weave and somewhat sheer, i.e., exhibit easily observed open space between yarns, in order to mitigate the effects of near contact between adjacent yarns of the same yarn system. The fabric constructions are 30.0 by 26.4, 30.0 by 25.6, and 28.7 by 14.6, warp yarns/cm by filling yarns/cm, and the areal densities are 113 g/m^2, 107 g/m^2, and 83.0 g/m^2, for the cotton, cotton/polyester, and polyester fabrics, respectively. The microstructural properties pertaining to the present tear propagation experiments are given in Table 1.

The results of tear propagation experiments are given in Table 2 for initial slit-like damage consisting of 35 and 45 breaks. Standard deviations are determined based on approximate formulas for propagation of error in calculated quantities (Taylor, 1990), where the variability of p_c, p_u, and f has been taken into account. Most of the variability exhibited by $\hat{p}_c$ stems from variability in f. The measurement of f is difficult, particularly for the staple yarn fabrics. For each case, three measurements of f, three measurements of p_c and three to six measurements of p_u were made.

Comparison of Analytical and Experimental Results

The experimental results given in Table 2 are plotted with the predictions made using our large-slit analysis for 35 and 45 breaks

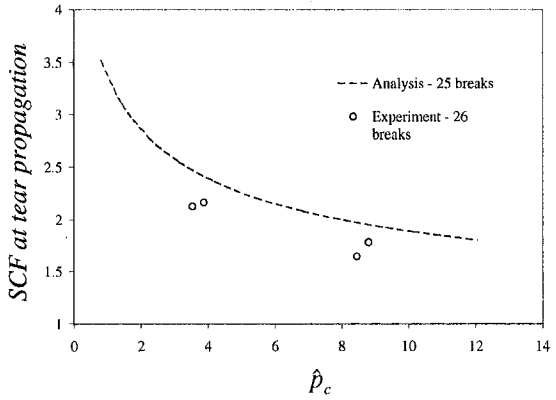

Fig. 10 Comparison of analytical 25 break slit SCF_{tp} versus $\hat{p}_c$ behavior with experimental results for 26 break slits given in Godfrey and Rossettos (1999)

in Fig. 9. The experimental and analytical results are seen to be in good agreement. In Fig. 10, preliminary experimental results given by Godfrey and Rossettos (1999) for 26 breaks are plotted with the analytical curve for 25 breaks (the present model has only been implemented for odd numbers of breaks). For this case, the analytical SCF_{tp} is consistently higher than that measured, suggesting two possibilities: (1) the 26 break slit is not sufficiently large to be well approximated by our large-slit approach; and (2) the smaller specimen size used in the earlier work affects the experimental results.

Conclusions

A simple micromechanical model has been developed to predict the onset of tear propagation at slit-like damage sites in biaxially stressed plain weave fabrics under increasing loading perpendicular to the line of breaks. The analysis has been specialized for large slits parallel to a yarn direction, where it is assumed that slip occurs at crossover points in a region along the first few intact yarns near the tip of the slit. The simplified slipping configuration applies to slits involving greater than, say, 35 breaks, where it can be shown a posteriori that the slip mechanism assumed in the analysis is the one that dominates for remote load values of interest. Experimental results have been presented for the onset of tear propagation in a variety of stressed cotton and polyester fabrics containing 35 and 45 break slits that agree well with predictions made using the present large-slit analysis.

References

Abbott, N. J., and Skelton, J., 1972, "Crack Propagation in Woven Fabrics," *Journal of Coated Fibrous Materials,* Vol. 1, pp. 234–252.

Christoffersen, J., 1980, "Fabrics: Orthotropic Materials With a Stress-Free Shear Mode," ASME JOURNAL OF APPLIED MECHANICS, Vol. 47, pp. 71–74.

Godfrey, T. A., 1998, "A Micromechanical Model for Damage Growth in Stressed Plain Weave Fabrics," Doctoral dissertation, Department of Mechanical, Industrial and Manufacturing Engineering, Northeastern University, Boston, MA.

Godfrey, T. A., and Rossettos, J. N., 1998, "Damage Growth in Prestressed Plain Weave Fabrics," *Textile Research Journal,* Vol. 68, pp. 359–370.

Godfrey, T. A., and Rossettos, J. N., 1999, "A Parameter for Comparing the Damage Tolerance of Stressed Plain Weave Fabrics," *Textile Research Journal,* Vol. 69, pp. 503–511.

Harrison, P. W., 1960, "The Tearing Strength of Fabrics," *Journal of the Textile Institute,* Vol. 51, pp. 91–131.

Hedgepeth, J. M., 1961, "Stress Concentrations in Filamentary Structures," NASA Technical Note D-882.

Koerner, R. M., Hwu, B., and Wayne, M. H., 1987, "Soft Soil Stabilization Designs Using Geosynthetics," *Geotextiles and Geomembranes,* Vol. 6, pp. 31–51.

Popova, M. B., and Iliev, V. D., 1993, "Simulation of the Tearing Behavior of Anisotropic Geomembrane Composites," *Geotextiles and Geomembranes,* Vol. 12, pp. 729–738.

Rossettos, J. N., and Godfrey, T. A., 1998, "Damage Analysis in Fiber Composite Sheets and Uncoated Woven Fabrics," ASME *Applied Mechanics Reviews,* Vol. 51, pp. 373–385.

Rossettos, J. N., and Olia, M., 1995, "On the Hybrid Effect and Matrix Yielding at Fibre Breaks in Hybrid Composite Sheets," *Mechanics of Composite Materials and Structures,* Vol. 2, pp. 275–280.

Rossettos, J. N., and Shishesaz, M., 1987, "Stress Concentration in Fiber Composite Sheets Including Matrix Extension," ASME JOURNAL OF APPLIED MECHANICS, Vol. 54, pp. 723–724.

Taylor, J. K., 1990, *Statistical Techniques for Data Analysis,* Lewis Publishers, Chelsea, MI.

Topping, A. D., 1961, "An Introduction to Biaxial Stress Problems in Fabric Structures," *Aerospace Engineering,* Vol. 20, pp. 18–19 and 53–57.

Troost, G. H., and Ploeg, N. A., 1990, "Influence of Weaving Structure and Coating on the Degree of Mechanical Damage of Reinforcing Mats and Woven Geogrids Caused by Different Fills During Installation," *Proc. 4th Int'l Conference on Geotextiles, Geomembranes and Related Products,* Vol. 2, G. den Hoedt, ed. A. A. Balkema, Rotterdam.